JOURNAL OF MATERIALS SCIENCE **35** (2000) 3213–3219

Role of preheating and specific energy input on the evolution of microstructure and wear properties of laser clad Fe-Cr-C-W alloys

J. CHOI
Center for Laser Aided Intelligent Manufacturing, Department of Mechanical Engineering & Applied Mechanics, University of Michigan, Ann Arbor, Michigan, USA

S. K. CHOUDHURI
Steel Authority of India, Ranchi, India

J. MAZUMDER
Center for Laser Aided Intelligent Manufacturing, Department of Mechanical Engineering & Applied Mechanics, University of Michigan, Ann Arbor, Michigan, USA

Synthesis of Fe-Cr-C-W alloy (10 : 4 : 1 : 1, wt(%)) was carried out on AISI 1016 steel substrate using laser cladding technique which lead to the development of a suitable alternate for cobalt bearing wear resistant alloys. This study involved understanding of process variables like preheating temperature and specific energy input on the evolution of microstructures and their effect on wear resistance properties. The microstructure was examined with a scanning electron microscope and various types of complex carbides were identified using both energy dispersive x-ray and auger spectroscopy facilities. A combination of MC, M_7C_3 and M_6C types of carbides of certain proportions (formed at a preheating temperature of 484°C with specific energy input of 9.447 KJ/cm^2) has been found to be most attractive for achieving an optimum combination of microhardness and steady state friction coefficient values. A similar advantage may be derived at a lower level of specific energy input of 8.995 KJ/cm^2 but with a higher preheating temperature of 694°C. However, increasing the specific energy input to 12.376 KJ/cm^2 can significantly soften the matrix.

1. Introduction

Development of new alloys by the laser cladding technique is found to be attractive particularly because of its inherent capability to overcome the limitations related to equilibrium thermodynamics and thereby facilitating commercial production of many new generations of synthetic materials with attractive property. The process is intensely dependent on energy input rate, momentum and mass transport phenomena and therefore the extent of mixing and final chemistry of clad zone is essentially controlled by its temperature gradient induced surface tension driven flow.

In the past synthesis of Fe-Cr-Mn-C alloy was reported [1–3] with a view to understand the formation of various types of carbides and nonequilibrium phases and their effect on wear resistance properties. Encouraging results from previous studies have provided an incentive to explore other improved wear resistance material, Such as Fe-Cr-C-W system [4]. Previous studies of Fe-Cr-C-W have proved that crack-free clad can be achieved using preheating techniques, and has shown that Fe-Cr-C-W system gives better wear properties than that of Stellite 6 and Fe-Cr-Mn-C [4]. The present study is therefore designed to understand how processing parameters like preheating temperature and specific energy input can influence the formation of various types of complex carbides and their interaction with the wear resistance property. Such information will ultimately lead to the process optimization for production of defect free alloy with good combinations of wear, hardness and toughness property.

2. Experimental procedure

The experimental setup (Fig. 1) comprises of three units, namely the laser source, powder dispenser and a preheating furnace. In the present investigation an AVCO HPL 10 KW continuous wave CO_2 laser with F7 Casegrain optics was used to produce doughnut-shaped beam with a Gaussian power distribution in the outer ring and none at the hole of the doughnut. The laser was operated at a power output of 3 to 4 KW. Specimens were traversed relative to the laser beam at a speed varied from 10.58 to 11.85 mm sec^{-1}. The corresponding specific heat input energy was in the range of 9.4475 to 12.376 KJ/cm^2. The laser power density and interaction time were 25–44.4 KW/cm^2 and 0.2531–0.3779 sec, respectively.

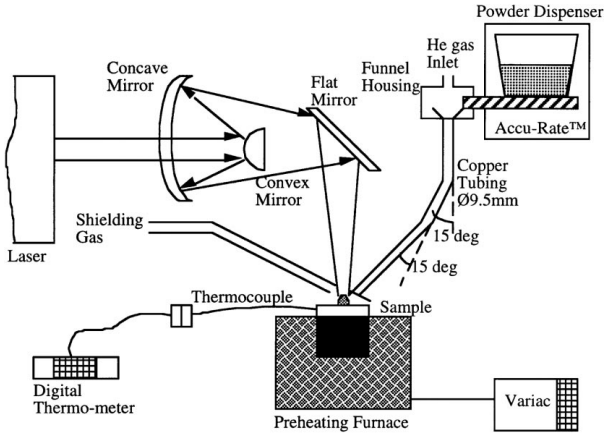

Figure 1 Experimental setup for laser cladding.

The powder was delivered to the area of interaction by a pneumatic powder delivery system with a feed screw and flow of powder was regulated at a fixed rate of 0.5368 gm/sec by injecting a small amount of helium gas continuously through the tube along with the powder. It may be mentioned that the direct placement of powder for cladding into the molten pool is beneficial over the preplaced cladding procedure, for achieving optimum specific energy needed for cladding and refinement of microstructure [5]. During cladding surface contamination was minimized by using helium as shielding gas. Helium has higher ionization potential compared to argon gas and thus produces plasma with lower electron density at the laser-substrate interaction point. Loss of laser energy due to inverse Bremsstrahlung absorption at the plasma column increases with the increasing electron density. Elemental powders like Fe, Cr, C and W of specific size range and purity were mixed together in the weight ratio of 10 : 4 : 1 : 1 as shown in Table I. The mixed powder was then dried at 200°C in a tube furnace with a steady flow of argon gas for about eight hours followed by slow cooling to ambient temperature.

TABLE I Size and purity of the element powders

Element	Size (μm)	Purity (%)	wt (%)	at (%)
Fe	6–9	99.9	62.5	51.9
Cr	2	99.5	25.0	22.3
C	0–300 mesh	99.5	6.25	24.2
W	0.5	99.9	6.25	1.60

Preheating of base material (substrate) fabricated from AISI 1016 steel with 6.35 mm (1/4 in) thickness were carried out on an electrically heated platform. The temperature of substrate was carefully controlled by monitoring the output from a thermocouple fixed with the specimen at a mid thickness. Altogether five different preheating temperatures, e.g., 298°, 384°, 484°, 695°, and 725°C were selected for the present study with a fixed specific energy input of 9.4475 KJ/cm^2. Separately, some cladding were also made at a fixed preheating temperature of 694°C. When laser power input was varied from 3 KW to 4 KW, corresponding specific energy inputs were of the order of 8.9958 and 12.376 KJ/cm^2, respectively. Table II gives details of processing parameters followed in this investigation.

Characterization of microstructure in the transverse midsection of the clad layer was performed with the Scanning Electron Microscope (SEM) using the Energy Dispersive X-ray microanalysis (EDX) system. Additionally, the Auger Electron Spectroscope (AES) was used for semi-quantitative chemical analysis of individual phases.

Wear tests performed on a block-on-cylinder machine using standard disc made of AISI 52100 steel (R_c hardness 60) (Fig. 2). Rectangular test blocks were machined from the cladded composite leaving approximately 1.2 mm thick clad layer at the top surface. Each test was continued for one hour when disk was rotated at 24 rpm (0.032 m/sec). Using paraffinic mineral oil (Sunvice 21) as a lubricating media, all tests were

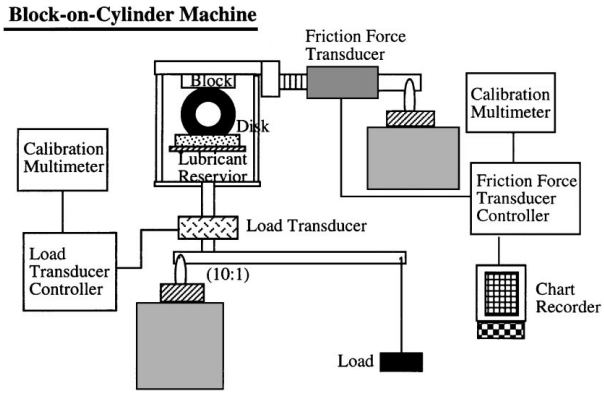

Figure 2 Schematic drawing for wear test.

TABLE II Laser cladding parameters for synthesis of Fe-Cr-C-W alloy

Sample #	Beam dia.[a] (mm)	Laser power (KW)	Traverse speed (mm/sec)	Powder feedrate (gm/sec)	Preheating temp.[b] (°C)	Specific energy (KJ/cm^2)	Power density (KW/cm^2)	Interaction time (sec)
16-1	4	4	10.58	0.5368	298	9.4475	25	0.3779
17-2	4	4	10.58	0.5368	384	9.4475	25	0.3779
19-1	4	4	10.58	0.5368	484	9.4475	25	0.3779
7-2	4	4	10.58	0.5368	698	9.4475	25	0.3779
7-3	4	4	10.58	0.5368	725	9.4475	25	0.3779
8-1	3	3	11.01	0.5368	694	8.9958	33	0.2726
8-2	3	4	11.85	0.5368	694	12.376	44.4	0.2531

[a]The laser beam diameter is OD, not ID.

[b]The preheating temperature was measured at the beginning of each process. Usually it increased up to 20–30°C from the initial value during the laser irradiation.

carried out at a fixed load (220 N) and wear properties were evaluated with steady state friction coefficient by eliminating the friction coefficient values up to sliding distance of initial 25 m. Vickers microhardness were assessed at the midsection of the clad zone for correlating them with the wear property.

3. Results

3.1. Microstructure

The overall microstructure of the laser melted zone are usually found to be uniform and fine grain. This has been possible due to formation of homogeneous liquid solution because of high mixing rate and very high degree of supercooling, approximately the same as for the rapid solidification process (RSP) (10^5 to 10^6°C/sec) [6, 7]. However, preheating of substrate would cause imposition of thermal imbalance in the melted zone and thereby creates an altered solidification characteristic with more modest coding rate leading to localized inhomogeneity in the microstructure. Fig. 3a and b are the scanning electron micrographs of laser cladded Fe-Cr-W-C alloy produced after preheating the substrate at 298°C, revealing the presence of three different constituents of phases. Namely, elongated (aligned), blocky/modular type, and featureless bright network of phase along the prior austenite grain boundaries. Increasing the preheating temperature to 384°C reduced the length of elongated phase significantly and appeared as much shorter aligned blocks which were surrounded by slightly less darker blocky/irregular type of phase (Fig. 4). Further increase in preheating temperature to 484°C showed reappearance of brighter phase but in an isolated form only at the grain boundaries of blocky/irregular phase (Fig. 5). Surprisingly, the microstructure at a much higher preheating temperature of 698°C showed presence of a single phase, which was somewhat like protruded blocky/irregular phases (Fig. 6). At the highest preheating temperature of 725°C, the microstructure was essentially composed of semi-elongated (aligned) and nodular form of phases with localized segregation of brighter phase trapped in between the nodules (Fig. 7).

The microstructural change at the laser melted zone on account of varied conditions of specific energy input/power density while cladding on a substrate preheated at 694°C was found to be significant. Fig. 8 shows the presence of very fine needle-shaped phases all over the melt zone produced at a specific energy input of 8.9958 KJ/cm^2 with corresponding power density of 33 KW/cm^2. Some of these needle shaped phases were brighter particularly those present at the junction of grains (Fig. 8). The situation became entirely different when specific energy input was raised to 12.376 KJ/cm^2 (corresponding power density −44.4 KW/cm^2). In this case the matrix was essentially comprised of very fine needle-shaped dendrites with large elongated/nodular phase embedded in it (Fig. 9).

Analysis of every individual phase had been carried out both by EDX and AES techniques and the results are shown in Tables III and IV. It may be noted that both the techniques are complementary to each other particularly when both heavier elements like W, Cr and Fe and lighter element C had to be analyzed.

3.2. Hardness and wear property

During wear test one would observe two different types of friction state, transient state and steady state. Initial friction coefficient for the preheated at 298°C was measured 0.164, at 484°C, 0.154, and at 698°C was measured 0.145, respectively (Fig. 10). Initial friction force was usually high and somewhat unstable until the disk turned smoothly after transient period. Then the friction force is stable and steady. The samples at preheating temperature, 698°C, showed higher transient/steady state friction coefficient than those at 298°C and 484°C.

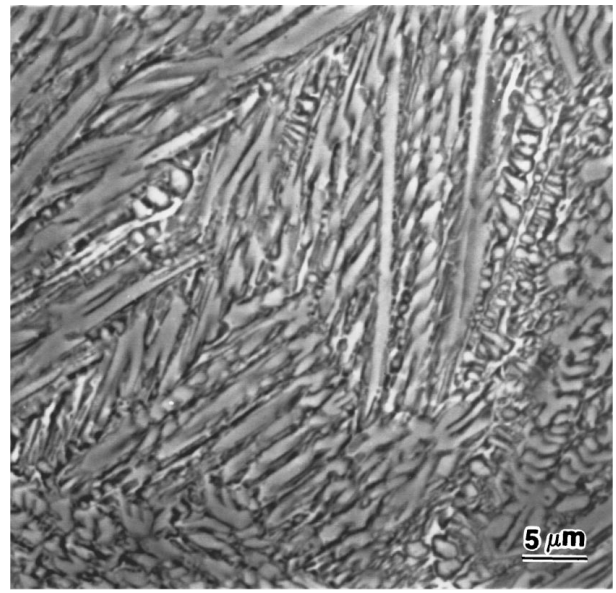

(a)

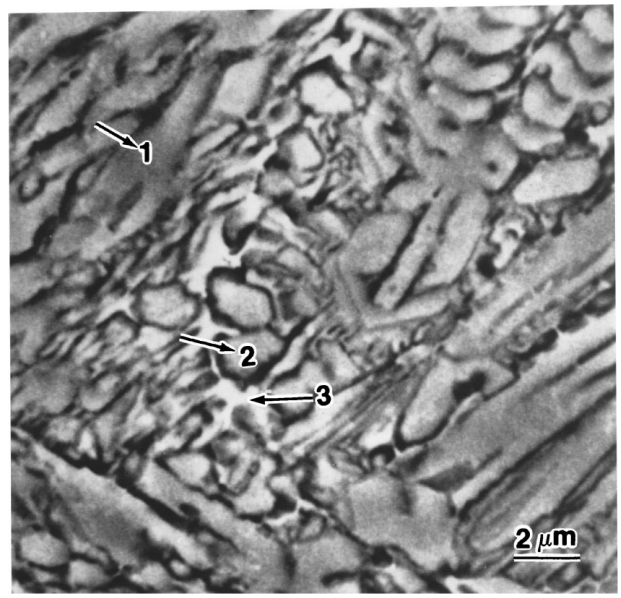

(b)

Figure 3 SEM micrograph of laser cladded zone (Sample#16-1; preheated at −298°C; specific energy ∼9.447 KJ/cm^2) SEM micrograph showing presence of amorphous phase (M_6C type carbide) at prior austenite grain boundaries (1-elongated (dark), 2-blocky-nodular (light), 3-bright smooth (interface)).

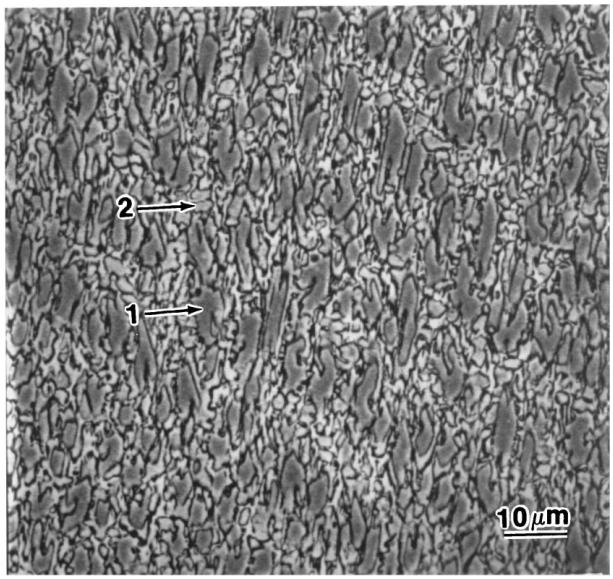

Figure 4 SEM micrograph of laser cladded zone (sample#17-2; preheated at 384°C; specific energy ∼9.447 KJ/cm^2; 1-semi elongated (dark), 2-blocky-nodular (light)).

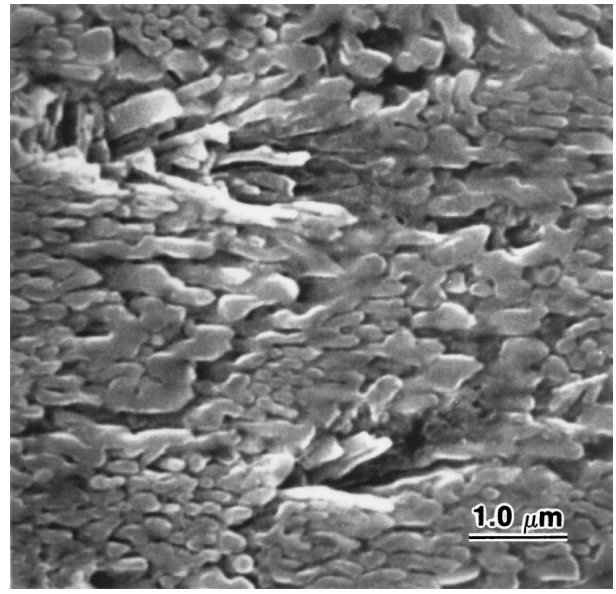

Figure 6 SEM micrograph of laser cladded zone (sample#7-2; preheated at 698°C; specific energy ∼9.447 KJ/cm^2; blocky/irregular).

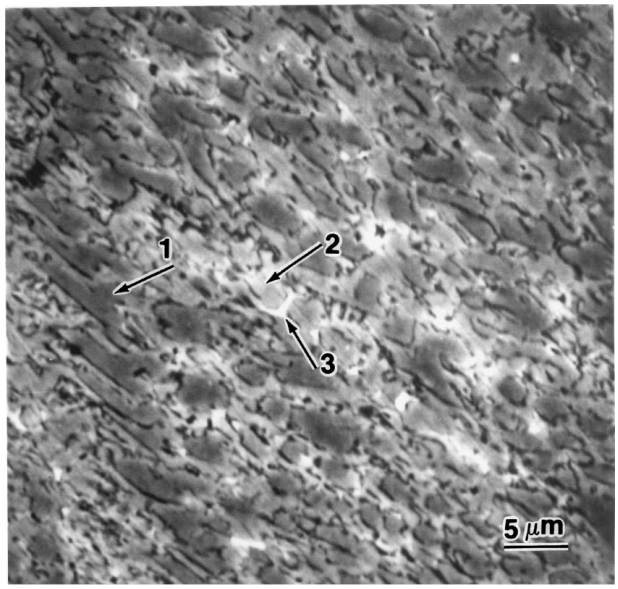

Figure 5 SEM micrograph of laser cladded zone (sample#19-1; preheated at 484°C; specific energy ∼9.447 KJ/cm^2; 1-elongated (dark), 2-blocky-irregular (light), 3-bright smooth (interface)).

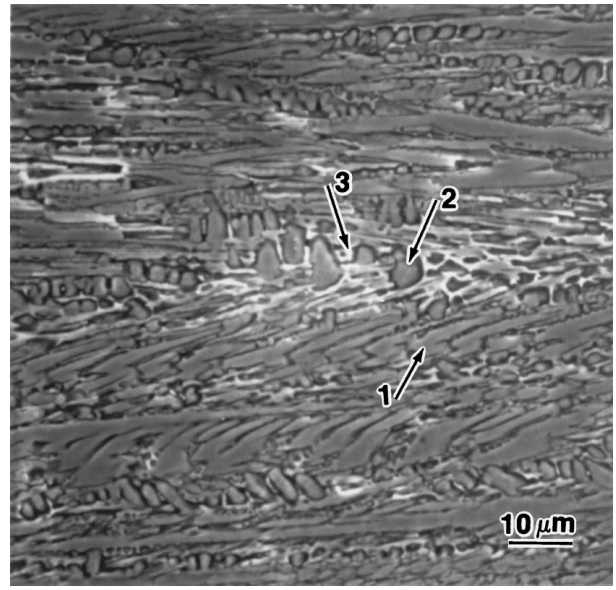

Figure 7 SEM micrograph of laser cladded zone (sample#7-3; preheated at 725°C; specific energy ∼9.447 KJ/cm^2; 1-semi elongated (dark), 2-blocky-nodular (light), 3-bright smooth (interface)).

Fig. 11 shows the microhardness distribution measured from the top surface under the same process parameters at the preheating temperature, 298°C, 398°C, and 725°C, respectively. The results show that average microhardness on the laser clad can be affected by the preheating temperature. The microhardness shows, in general, that hardness near the interface from clad is somewhat higher than that near the top surface of clad. Average microhardness for the preheating temperature, 298°C, was appeared higher than those for higher preheating temperature cases.

Uniformly high microhardness was observed at varied conditions of preheating. The steady state friction coefficient were nearly constant with the preheating temperature while microhardness followed some power law equation (Fig. 12). At a preheating temperature close to 490°C both microhardness and wear properties were found to be optimum (Fig. 12). Further, the microhardness of cladded zone produced with lower specific energy input (8.9958 KJ/cm^2) was found to be higher (H_v751) than that (H_v677) of higher specific energy input of 12.376 KJ/cm^2. Correspondingly the coefficient of steady state friction varied from 0.110 to 0.112.

4. Discussion

Microstructure of laser cladded Fe-Cr-C-W alloy showed the presence of different types of carbides in ferrite matrix and their types were predominantly controlled by the preheating temperature. If we examine the carbides formed at two extreme conditions of

TABLE III Atomic concentration of elements in various phases (SEM EDX analysis)

Sample #	Preheating temp (C)	Morphology	Approx. atomic concentration (%) Fe	Cr	W	C
16-1	298	Elongated (dark)	40.77	52.95	4.84	1.43
		Blocky-nodular (light)	74.56	19.35	5.63	0.46
		Bright smooth (interface)	35.05	25.80	37.75	1.40
17-2	384	Semi elongated (dark)	53.35	38.35	6.82	1.49
		Blocky-nodular (light)	74.54	20.62	4.25	0.58
19-1	484	Elongated (dark)	41.01	52.59	5.01	1.40
		Blocky/irregular (light)	80.26	14.49	4.84	0.41
		Bright smooth (interface)	56.85	13.10	29.55	0.51
7-2	698	Blocky/irregular	50.42	42.64	5.63	1.30
7-3	725	Semi elongated/nodules (dark)	81.24	15.51	2.35	0.91
		Blocky-nodular (light)	58.73	33.37	6.92	0.99
		Bright smooth (interface)	44.21	43.35	9.34	1.10
8-1	694	Needle shape (dark)	40.40	56.95	2.53	0.13
		Needle shape (bright)	40.76	55.41	3.64	0.19
8-2	694	Needle shape (light)	44.56	51.62	3.71	0.12
		Elongated/nodular (dark)	81.25	17.70	0.97	0.09

TABLE IV Summary of AES analysis

Sample #	Preheat *T* (°C)	Morphology	Element concentration % C1	O1	Cr2	Fe3	W1	Approx. chemistry % Metal	Carbon	Type of carbide predicted
16-1	298	Elongated (dark)	34.73	32.38	19.63	7.03	6.24	48.6	51.4	MC
		Blocky/nodular (light)	21.68	40.02	29.25	4.17	4. 88	63.9	36.1	M_2C
		Bright smooth (interphase)	35.09	21.19	18.56	4.44	20.72	55.5	44.5	M_6C_5
		Semi-elongated (dark)	52.77	8.20	18.78	20.25	—	43.0	57.0	MC
19-1	484	Blocky/irregular (light)	20.36	30.37	18.5	30.79	—	70.7	29.25	M_7C_3
		Bright smooth (interphase)	9.89	24.96	5.61	59.54	—	86.8	13.2	M_6C
		Semi-elongated/nodules (dark)	24.77	30.64	16.16	25.08	3.34	64.3	35.7	M_2C
7-3	725	Blocky/nodular (light)	18.81	28.17	3.58	47.15	2.29	73.8	26.2	M_3C
		Bright smooth (interphase)	29.0	17.12	6.37	26.17	21.34	65.0	35.0	M_2C
8-2	694	Semi-elongated (dark)	45.32	10.68	2.31	41.69	—	49.3	50.7	MC
		Blocky/irregular (light)	53.10	8.28	5.98	32.64	—	42.1	57.9	M_2C_3

All specimens sputtered for 10 minutes prior to analysis.

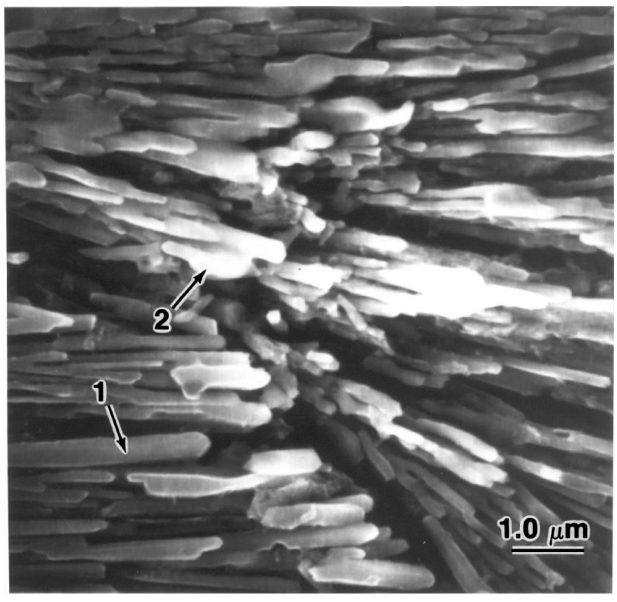

Figure 8 SEM micrograph of laser cladded zone (sample#8-1; preheated at 694°C; specific energy ~8.995 KJ/cm^2; 1-needle shape (dark), 2-needle shape (light)).

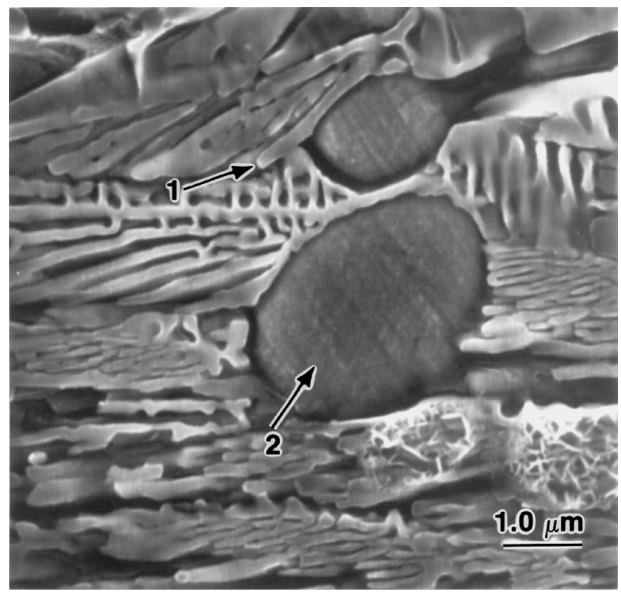

Figure 9 SEM micrograph of laser cladded zone (sample#8-2; preheated at 694°C; specific energy ~12.376 KJ/cm^2; 1-needle shape (light), 2-elongated/nodular (dark)).

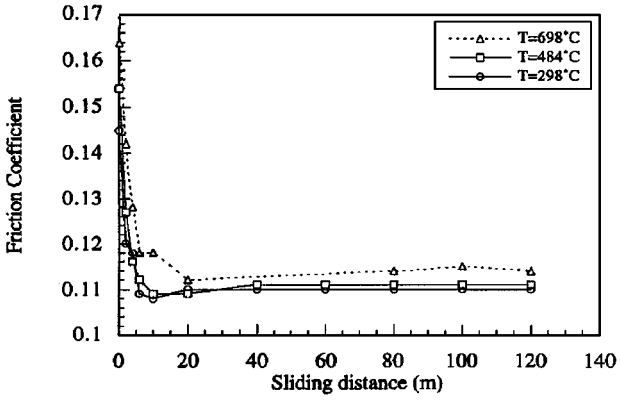

Figure 10 Comparison of friction coefficient with respect to sliding distance between two preheated samples ($T = 298°C$, $T = 484°C$, and $T = 698°C$) under same process parameters (laser power = 4 kW, beam dia. = 4 mm, traverse speed = 10.58 mm/sec, powder feedrate = 0.5368 gr/sec).

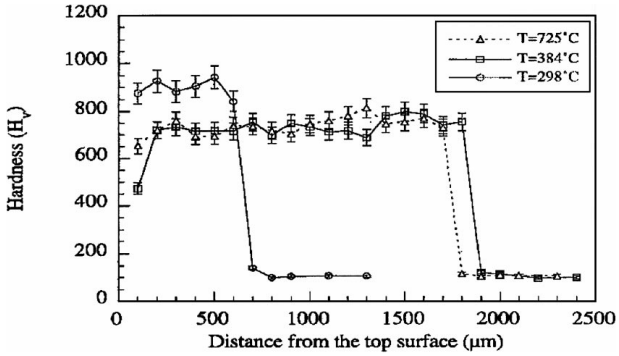

Figure 11 Comparison of microhardness (H_v) with respect to the preheating temperature ($T = 298°C$, $T = 384°C$, and $T = 725°C$) under same process parameters (laser power = 4 kW, beam dia. = 4 mm, traverse speed = 10.58 mm/sec, powder feedrate = 0 .5368 gr/sec).

preheating, i.e., 298° and 725°C (specific energy input being identical in both the situations), it can be seen that though the morphology of carbides appeared to be almost similar but the metal and carbon concentrations in them were remarkably different. Comparing the chemistry of a specific type of carbide morphology present in both the situations, the concentration of carbon was found to have reduced while metal content had raised with the increase in preheating temperature (Table IV). Moreover, the size of carbides were much coarser at the higher preheating temperature.

The appearance of featureless bright phases at various preheating conditions as continuous network at the prior austenite grain boundaries (Fig. 3a), isolated films at the grain boundaries of blocky/nodular type of carbides (Fig. 5) and aggregated in between the array of elongated carbides (Fig. 7) were due to the formation of deep eutectic enriched with W in particular and also with Cr (Table III). These phases were either M_6C_5, M_6C and M_2C types depending on relative concentration of metal and carbon. Each of these carbides can form only at a specific preheating temperature.

As the preheating was adopted to eliminate cracks perpendicular to cladding direction, the influence of preheating ought to be addressed. From the results, it is now clear that preheating temperature had profound influence on the evolution of various types of carbides

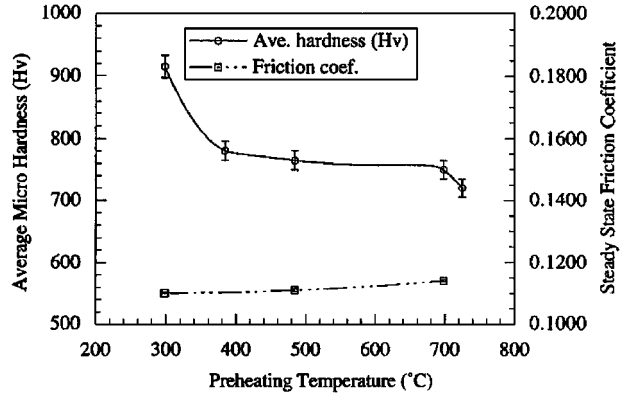

Figure 12 Variation of microhardness and steady state friction coefficient with respect to preheating temperature.

and also on their size and distribution. Therefore, it was obvious to expect a marked effect on hardness and wear properties. As shown in Fig. 10, the higher preheating temperature might contribute to increasing transient and steady state friction coefficient, since the size of carbides were more coarse as the preheating temperature goes higher. Wear properties usually depend upon the size of carbides in the matrix structure, since the carbide phases play a role of barrier while the matrix phases give damping effect [8]. In fact, the larger size of carbides resulted in increase of the wear resistance [4]. As the metal concentration in the carbide varies with preheating temperature, the microhardness in the carbide is also affected by preheating temperature. The high preheating temperature can enhance diffusion into the matrix, diluting the Cr/W-rich carbides such as MC. Consequently, the wear properties and microhardness properties were affected by the preheating temperature, however, influence of the preheating temperature was not so significant as specific energy. High preheating temperature can contribute to increase in the carbide size while low preheating temperature helps to keep microhardness high.

Fig. 12 shows the variation of microhardness and steady state friction coefficient with respect to preheating temperature. Microhardness property was affected by the preheating temperature, as expected. It was predictable, in some sense, since the morphology of carbides in this alloy might be altered with increasing preheating temperature. Meanwhile, it was also expected that the preheating temperature could influence friction properties, however it was found that preheating did not vary the magnitude of friction coefficient significantly.

Since the idea of preheating was to minimize and eventually eliminate the undesirable tensile residual stress in the clad [4], it was considered that the microstructure corresponding to the preheating temperature, 484°C, as comprised of MC, M_7C_3 and M_6C types of carbides in a ferrite matrix was favorable. Amongst these carbides MC type of carbide (enriched with both Cr and C) would probably be the most hard particle and M_6C type of carbide (higher concentration of W with moderate amount of Cr and C) would show slightly lower hardness relative to MC type carbide; whereas M_7C_3 type carbide (enriched with Fe and moderate amounts of Cr, W and C) is expected to be the most

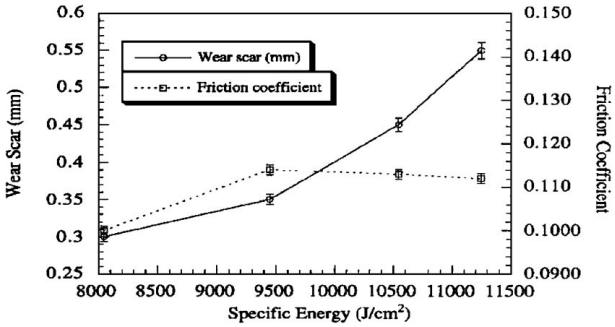

Figure 13 Variation of wear scar and steady state friction coefficient with respect to specific energy.

soft. The area fraction of MC and M_6C types of carbides was found to be around 45–50% (Fig. 6) which is perhaps an optimal mixture for achieving balanced wear and hardness properties with minimum defect.

Increasing the specific energy input can significantly reduce the cooling rate of the melt zone, while reverse is true with lowering of energy input [5]. Therefore, the net effect of variation in specific energy input would be somewhat similar to that of preheating situation. The microstructure produced with specific energy input of 8.995 KJ/cm^2 was much finer and hard (Fig. 8) compared to that produced with specific energy input of 12.376 KJ/cm^2 (Fig. 9). Interestingly, the wear and hardness properties of clad were produced at lower energy input (8.995 KJ/cm^2) with preheating temperature of 694°C can probably match with those produced with slightly higher energy input (9.447 KJ/cm^2) and maintaining preheating temperature of 484°C.

In case of former situation the carbides were mostly enriched with Cr and they were expected to be MC type where as for the latter condition the microstructure contained with MC, M_7C_3 and M_6C types of carbides.

The influence of the specific energy input on the size of wear scar was also plotted (Fig. 13). Similar to microhardness case, higher specific energy input produced larger size of wear scar, however, the steady state friction coefficient was appeared not that sensitive to the specific energy input. The morphology of carbide is more influential on the microhardness than on friction properties.

5. Summary

Synthetically produced Fe-Cr-C-W alloy using laser cladding technique was found to be an attractive alternative to the cobalt bearing alloys [9]. Preheating of substrate significantly altered the nature, size and distribution of carbides. Laser cladding with specific energy input of 9.447 KJ/cm^2 and maintaining preheating temperature at ∼500°C produced best possible combination of wear and hardness properties and the microstructure was comprised of MC, M_7C_3 and M_6C types of carbides (MC + M_6C ∼ 45–50%) with ferrite matrix. Increasing the specific energy input rate to a level of 12.376 KJ/cm^2, keeping the preheating temperature at 694°C; lead to the formation of much more coarse and soft microstructure whereas reverse was true for lower specific energy input of 8.995 KJ/cm^2. In the latter case the microstructure was essentially Cr rich MC type of carbides with ferrite matrix and the hardness and wear properties were similar to one produced with slightly higher specific energy input of 9.447 KJ/cm^2 with a preheating temperature of 484°C.

Acknowledgement

This work was made possible by a National Science Foundation Indo-US grant.

References

1. E. EIHOLZER, C. CUSANO and J. MAZUMDER, Proc. of the Int'l. Congress on Application of Lasers and Electro-optics, Boston, MA, Vol. 44, edited by J. Mazumder (Laser Institute of America, Nov. 1984) p. 159.
2. J. SINGH and J. MAZUMDER, *J. Mat. Sci. and Tech.* **2** (1986) 709.
3. *Idem., Met. Trans. A* **18A** (1987) 313.
4. J. CHOI and J. MAZUMDER, *J. Mat. Sci and Tech.* **29** (1994) 4460.
5. L. J. LI and J. MAZUMDER, in Laser Processing of Materials edited by K. Mukherjee and J. Mazumder (Proc. of the Metal. Soc. AIME, Warrendale, PA, 1984) p. 35.
6. T. CHANDE and J. MAZUMDER, *J. of Appl. Phys.* **1** (1982).
7. N. M. WEERASINGHES and W. M. STEEN, "Transport Phenomena in Materials Processing," Vol. 1, edited by M. M. Chen, J. Mazumder and C. L. Tucker (ASME, 1983) p. 15.
8. D. A. RIGNEY, (ed) Fundamentals of Friction and Wear of Materials, ASM, Papers presented at the 1980 ASME Materials Science Seminar, p. 73.
9. J. MAZUMDER, J. CHOI, C. RIBAUDO, A. WANG and A. KAR, "Non-Equilibrium Synthesis of Alloys Using Lasers," International Conference on Beam Processing of Advanced Materials edited by J. Singh and S. M. Copley (TMS, 1993) p. 41.

Received 11 August
and accepted 10 December 1999